JOURNAL OF COMPUTATIONAL PHYSICS **143,** 665–673 (1998)
ARTICLE NO. CP985979

NOTE

On the Termination of the Perfectly Matched Layer with Local Absorbing Boundary Conditions[1]

1. INTRODUCTION

Unsplit [4–5] perfectly matched layers (PML, see [1] for the original split-field formulation) have proven to be effective alternatives to local absorbing boundary conditions (ABC) for the truncation of computational domains employed in the numerical solution of electromagnetic wave propagation problems. The PML ($0 \le z < d$) is placed adjacent to a computational domain Ω_c ($z < 0$) and is truncated at $z = d$ by imposing a homogeneous Dirichlet boundary condition on the tangential Electric fields there, e.g., $B = 1$ in Fig. 1. This is equivalent to enclosing the computational domain with a metal (perfect electric conductor, or PEC) box whose inner walls are coated with a wave absorber of depth d and loss profile $\sigma(s)$, where s is the depth coordinate into the layer. The electric and magnetic conductivities in the layer are then proportional to $\sigma(s) = \sigma_{\max} s^n$, where $n = 0, 1, 2$, the constants of proportionality being the permittivity ϵ and permeability μ, respectively. In applications the layer is tuned by varying $\sigma_{\max}$ to achieve the maximum absorption of outgoing waves for given d and discretization parameters. A properly tuned layer typically provides more than 3 orders of magnitude reduction in spurious reflection due to artificial grid truncation over that afforded by classical approaches. Therefore, it is of interest to explore the possibility of further improving such performance by altering the boundary condition used to terminate it. Previous work on terminating the Berenger PML with local ABCs [2, 3] did not take into account the presence of loss in the layer and only examined the reflection properties of the composite layer obtained with operators B derived for the *lossless* wave equation. Consequently, little improvement was evident with those approaches leaving the hope that more improvement can be realized if the loss *is* taken into account.

Herein, using as a starting point the two-dimensional unsplit PML equations [4, 5] for the TM polarization in a layer that is perpendicular to the $\hat{z}$-axis [5], we derive and implement

[1] The U.S. Government's right to retain a nonexclusive royalty-free license in and to the copyright covering this paper, for government purposes, is acknowledged.

0021-9991/98 $25.00

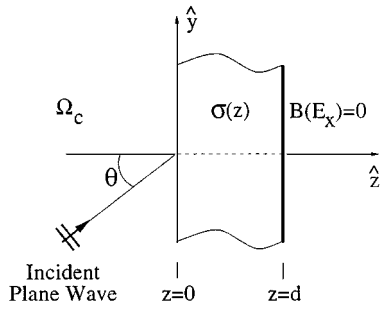

FIG. 1. The PML geometry.

two local ABCs, which take into account the loss in the layer, to replace the PEC termination. We also derive the analytical reflection coefficients of the composite layer. Our first-order ABC is equivalent to setting the incoming characteristic variable equal to zero at $z = d$, and thus it is particularly useful for staggered schemes [6] for which characteristic boundary conditions cannot be readily implemented due to the dependent variables not being colocated in space-time.

We test the resulting combinations by determining the reflection of outgoing waves obtained with the ABC-backed layer in a simulation of scattering of transient cylindrical waves by a dielectric cylinder in two dimensions and comparing it to the reduction obtained with a PEC-backed layer. We find that using the ABC-backed layer in transient numerical simulations is justified only for the $n = 0$ conductivity case (constant loss profile), while for the $n = 1, 2$ cases (linear or quadratic conductivity variation) we find that the ABC-backed layer performs as well as the simpler, PEC-backed, layer. Hence, we conclude that *it is not worthwhile* to replace the simple PEC backing of the PML with other, computationally more expensive procedures when the time-domain wavefields to be absorbed are wideband. We caution the reader that our work herein does not determine whether the ABC-backed layer is superior to the PEC-backed layer for monochromatic time-harmonic problems.

2. DERIVATION

A plane wave of frequency ω is incident at an angle θ on a PML layer (see Fig. 1) placed adjacent to the computational domain Ω_c. The fields in Ω_c satisfy the two-dimensional Maxwell equations (TM-polarization, $e^{i\omega t}$ time dependence, scaled for convenience so that $\epsilon = \mu = 1$)

$$
\begin{aligned}
i\omega E_x &= \frac{\partial H_z}{\partial y} - \frac{\partial H_y}{\partial z} \\
i\omega H_y &= -\frac{\partial E_x}{\partial z} \\
i\omega H_z &= \frac{\partial E_x}{\partial y}.
\end{aligned}
\tag{2.1}
$$

The electromagnetic waves in the PML are modeled by the modified Maxwell equations [5]

$$\begin{aligned} i\omega\left(1 - i\frac{\sigma(z)}{\omega}\right)E_x &= \frac{\partial H_z}{\partial y} - \frac{\partial H_y}{\partial z} \\ i\omega\left(1 - i\frac{\sigma(z)}{\omega}\right)H_y &= -\frac{\partial E_x}{\partial z} \\ i\omega\frac{H_z}{\left(1 - i\frac{\sigma(z)}{\omega}\right)} &= \frac{\partial E_x}{\partial y}. \end{aligned} \tag{2.2}$$

Electromagnetic arguments dictate that the tangential fields, E_x and H_y, are continuous at $z = 0$, while a boundary condition should be imposed on E_x at $z = d$, i.e., $B(E_x) = 0$. For transient waves in the layer we consider three boundary conditions

$$B_0 = 1, \tag{2.3}$$

and

$$B_m = \prod_{i=1}^{m}\left(\frac{\partial}{\partial t} + \frac{1}{\alpha_i}\frac{\partial}{\partial z} + \sigma(d)\right); \qquad m = 1, 2, \tag{2.4}$$

where $\alpha_i = \cos\theta_i$, $i = 1, 2$ are the cosines of the angles of perfect absorption for plane waves incident on the layer at $z = 0$ as they exit Ω_c.

The solution of (2.1) for the tangential fields in Ω_c is

$$\begin{pmatrix} E_x \\ H_y \end{pmatrix} = \begin{pmatrix} 1 \\ \alpha \end{pmatrix} e^{i\omega(t-\alpha z-\beta y)} + \begin{pmatrix} R_i \\ -\alpha R_i \end{pmatrix} e^{i\omega(t+\alpha z-\beta y)}, \tag{2.5}$$

where $\alpha = \cos\theta$ and $\beta = \sin\theta$. The unknowns R_i, $i = 0, 1, 2$ are the layer's reflection coefficients corresponding to each boundary condition (2.3)–(2.4).

The solution of (2.2) is easily obtained despite the variable coefficient $\sigma(z)$. In the layer region, $0 \le z < d$, it is

$$\begin{pmatrix} E_x \\ H_y \end{pmatrix} = \begin{pmatrix} A \\ -\alpha A \end{pmatrix} e^{i\omega(t+\alpha z+\alpha I(z)-\beta y)} + \begin{pmatrix} B \\ \alpha B \end{pmatrix} e^{i\omega(t-\alpha z-\alpha I(z)-\beta y)} \tag{2.6}$$

with $I(z) = \int_0^z \sigma(s)\,ds$.

The three unknowns R_i, A, and B are determined by applying the tangential-field continuity conditions at $z = 0$ and the boundary condition (with $\partial/\partial t$ replaced by $i\omega$) on E_x at $z = d$. We obtain the reflection coefficients

$$R_0 = -e^{-2i\omega\alpha-2\alpha I(d)}, \tag{2.7}$$

$$R_1 = -\frac{1 - \frac{\alpha}{\alpha_1}}{1 + \frac{\alpha}{\alpha_1}}R_0, \tag{2.8}$$

and

$$R_2 = -\frac{(i\omega + \sigma(d))^2\left(1 - \frac{\alpha}{\alpha_1} - \frac{\alpha}{\alpha_2} + \frac{\alpha^2}{\alpha_1\alpha_2}\right) - \sigma'(d)\frac{\alpha}{\alpha_1\alpha_2}}{(i\omega + \sigma(d))^2\left(1 + \frac{\alpha}{\alpha_1} + \frac{\alpha}{\alpha_2} + \frac{\alpha^2}{\alpha_1\alpha_2}\right) + \sigma'(d)\frac{\alpha}{\alpha_1\alpha_2}}R_0, \tag{2.9}$$

where $\sigma'(z) = \frac{d\sigma(z)}{dz}$. Our R_0 is Berenger's result for the PEC-backed layer; $R_0 \to 0$ as $d \to \infty$. Note that (2.8) shows that the finite layer behaves as an infinite layer ($R_1 \equiv 0$) for plane waves incident at $\theta = \theta_1$. Further, (2.9) shows that a constant finite layer (one for which $\sigma'(z) = 0$, $0 \le z \le d$) also behaves as an infinite layer for plane waves now incident at two angles, $\theta = \theta_1$ and $\theta = \theta_2$. Significantly, the dependence of R_2 on the general loss profile and its rate of change at $z = d$ indicates that the PML backed by local high-order ABCs ($m \ge 2$) *should not* result in any improvement over that afforded by the PEC-backed layer.

3. NUMERICAL EXPERIMENTS AND DISCUSSION

We now briefly discuss the implementation of (2.3)–(2.4) with a 2nd-order accurate staggered scheme [6] to solve (2.1)–(2.2) in the time domain. The application of (2.3) in the staggered scheme is trivial as one simply sets $E_x = 0$ by zeroing the electric field nodes placed at $z = d$. Each member of (2.4) is approximated here as

$$\frac{\partial}{\partial t} + \frac{1}{\alpha_i}\frac{\partial}{\partial z} + \sigma(d) \approx \frac{\left(1 - S_t^{-1}\right)\left(1 + S_z^{-1}\right)}{2\Delta t} + \frac{\left(1 - S_z^{-1}\right)\left(1 + S_t^{-1}\right)}{2\Delta\alpha_i} + \sigma(d)\frac{\left(1 + S_z^{-1}\right)\left(1 + S_t^{-1}\right)}{4}, \tag{3.1}$$

where the shift operators are defined in [7], and Δt and Δ are, respectively, the time- and spatial-step sizes. A composition of (3.1) is used to apply (2.4) to the update of the discrete E_x field on the boundary nodes at $z = d$ in order to provide the boundary closure for the scheme. The numerical order of accuracy of that closure is $O(\Delta^2)$ when the stability condition, $\Delta t \le \Delta/\sqrt{2}$, of the interior scheme is satisfied.

The numerical experiments involve a circular dielectric scatterer, illuminated by a cylindrical wave generated with a *pulsed* electric–current point source (see [5] for details of the setup), embedded in free space. The finite-sized computational domain Ω_c contains the source and the target, and is itself embedded inside a much larger reference domain Ω_L with boundary $\partial\Omega_L$ on which we implement a PEC condition. Domain Ω_c is truncated by surrounding it with a uniform width PEC-backed or ABC-backed PML. We consider two fixed layer widths, $d = 8\Delta$ and $2d = 16\Delta$ with $\Delta = 5 \times 10^{-3}$ corresponding to the coarsest spatial cell size used in the computations. As $\partial\Omega_L$ is placed sufficiently far from $\partial\Omega_c$, all points in the test domain are causally isolated from reflections generated at $\partial\Omega_L$ over the computation time interval $[0, T = 5t_s]$. To test and compare the two boundary treatments we compute the error

$$e(n\Delta t) = \left\| E_x^{\Omega_c}(\cdot, \cdot, n\Delta t) - E_x^{\Omega_L}(\cdot, \cdot, n\Delta t) \right\|_2; \qquad n \in [0, T/\Delta t], \tag{3.2}$$

introduced at each time step n by the artificial truncation of Ω_c. In (3.2), $E_x^{\Omega_c, \Omega_L}$ is the computed electric field in the appropriate domain indicated by the superscript, and the L_2 norm is taken over $\Omega_c \cup \partial\Omega_c$; this definition is a measure of how well the artificial truncation approximates the true "physics" at the boundary which dictates that there should be no boundary felt by the outgoing waves. The loss profile is tuned by varying $\sigma_{\max}$ to give the least reflection for the PEC-backed layer at the coarsest Δ for all n at a CFL number of 0.5. For Figs. 2–6 it turned out that this optimal $\sigma_{\max}$ was also optimal for the ABC-backed layer.

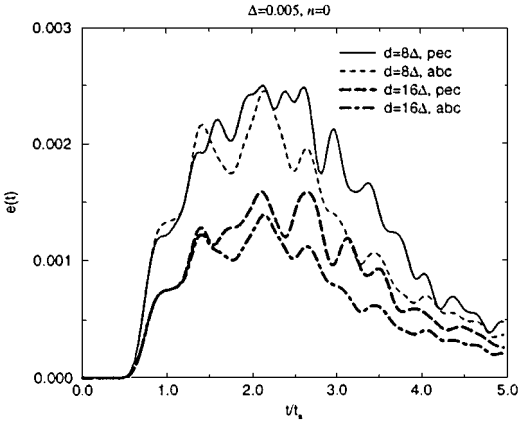

FIG. 2. Time dependence of the reflected energy due to the domain truncation.

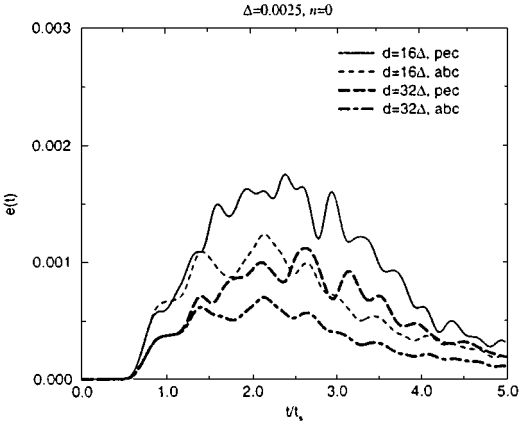

FIG. 3. Same as Fig. 2.

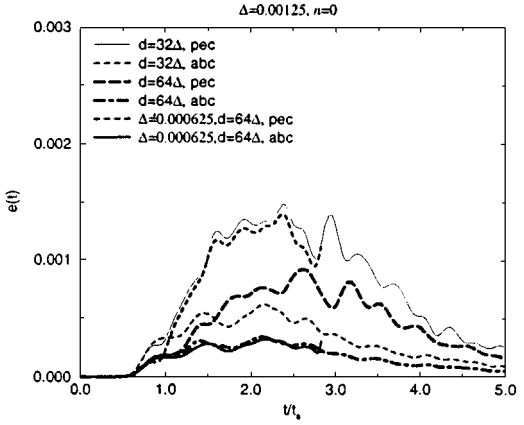

FIG. 4. Same as Fig. 2.

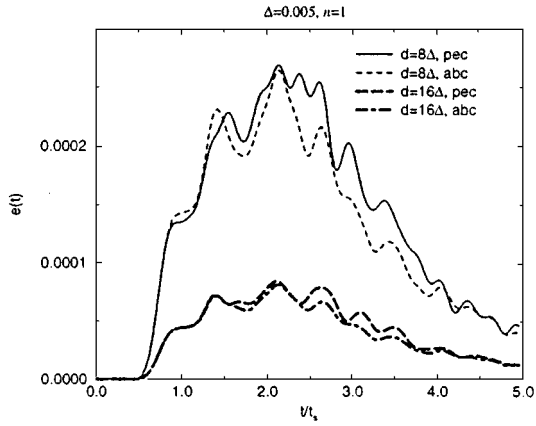

FIG. 5. Same as Fig. 2 for the linear layer.

We first experimented with $\alpha_1 = 1$ in the B_1 operator. Figures 2–4 summarize our findings for the 8-point versus the 16-point constant conductivity $n = 0$ layers. It is seen that the ABC-backed PML of width d performs as well as the PEC-backed PML on *coarse* grids (Fig. 2); as the grid is refined the ABC-backed layers outperforms the PEC-backed layer (Fig. 3). The ABC-backed layer of width d performs as a PEC-backed layer of width $2d$. Significantly, the reflection of the ABC-backed layer continues to decrease as Δ is refined, while that of the PEC-backed layer does not improve past a certain Δ (Fig. 4). This is because R_0 is a lower bound for all α in the PEC-backed computation, while for some α in the ABC-backed computation the corresponding lower bound is exactly zero. In Fig. 4, the finest resolution results where truncated at the time step past which they were contaminated by reflections from $\partial\Omega_L$ which were unavoidable due to computer memory limitations.

Figures 5 and 6 confirm that the ABC- and PEC-backed layers perform equivalently for the linear and quadratic variation loss profiles, respectively. They also show (note the change in the vertical scale) that merely increasing the degree of smoothness of the loss profile in the neighborhood of $z = 0$ eliminates the need for a sophisticated boundary treatment to truncate

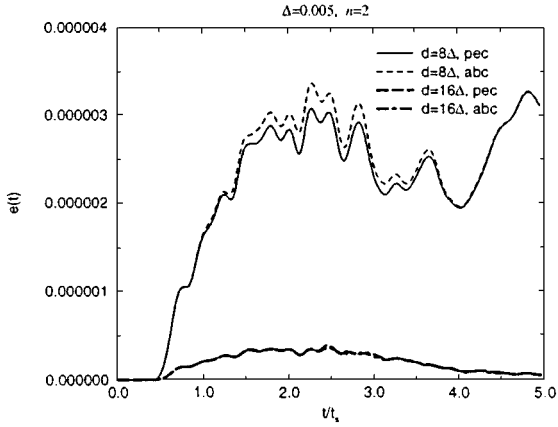

FIG. 6. Same as Fig. 2 for the quadratic layer.

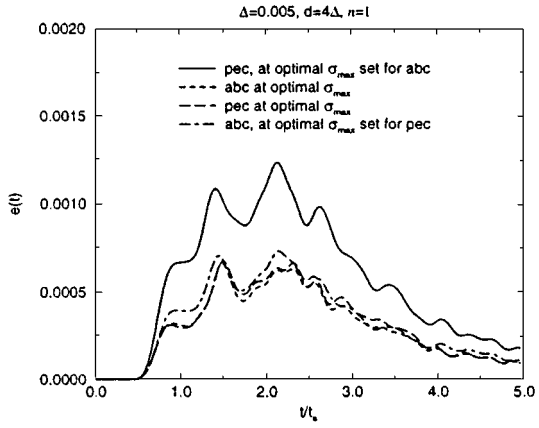

FIG. 7. The effect of the optimal σ for the two different backings.

the PML at $z = d$ as the reflection error is reduced by one and three orders of magnitude, respectively, from its maximum value attained with $n = 0$ at the same discretization. We have also experimented with other values of $0 < \alpha_1 < 1$ but our best results did not improve further.

To test the inference of the previous paragraph we also experimented with an $n = 1$ layer of width $d/2 = 4\Delta$ at the coarsest spatial step. We found that the optimal $\sigma_{\max}$ for the PEC-backed layer was non-optimal for the ABC-backed layer which required further tuning to $\sigma_{\max}^{\mathrm{ABC}} \approx 1.5 \times \sigma_{\max}^{\mathrm{PEC}}$; the additional dispersion introduced by the ABC termination is important for shallow layers only. Figure 7 shows that merely changing the type of termination of an optimal (obtained by varying $\sigma_{\max}$) PEC-backed layer does not result in an improvement; actually, the ABC-backed layer at this width and $\sigma_{\max}$ is slightly worse. However, an optimal ABC-backed layer produces about half the reflection of the PEC-backed layer of the same width operated at the same $\sigma_{\max}$. Using these two sets of runs as a baseline we then refined the grid once ($\Delta = 0.0025$). Figure 8 shows that, for fixed layer

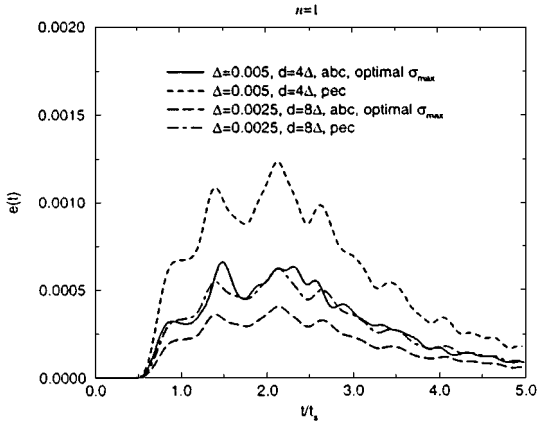

FIG. 8. Time dependence of the reflected energy due to the domain truncation with the optimized ABC-backed PML.

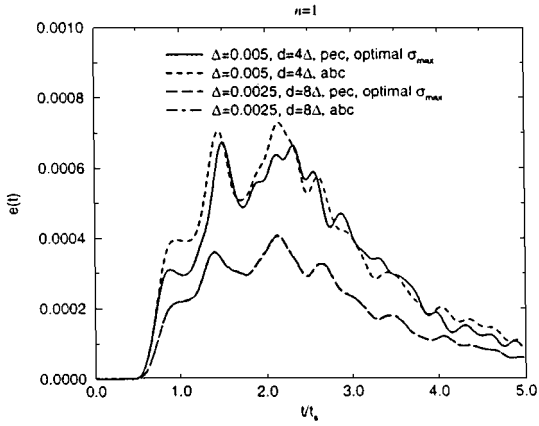

FIG. 9. Same as Fig. 8 for the optimized PEC-backed PML.

width, a tuned ABC-backed layer outperforms the PEC-backed layer when it is operated at the same (non-optimal) $\sigma_{\max}$. On the other hand, when the PEC-backed layer is optimal merely replacing the termination does not result in an improvement (Fig. 9).

We also tested the B_2 operator with $\alpha_1 = \alpha_2 = 1$. The results were indistinguishable from those obtained with the PEC-backed layer for all n. Other choices for α_1 and α_2 in the interval (0, 1] produced poorer results.

We conclude that, in the framework herein, *it is not worthwhile* to replace the PEC boundary condition, typically used to truncate the perfectly matched layer, with one that is computationally more expensive.

ACKNOWLEDGMENT

This research was sponsored by the Air Force Office of Scientific Research, Air Force Materials Command, USAF, under Grant F49620-98-1-0001. The views and conclusions contained herein are those of the author and should not be interpreted as necessarily representing the official policies or endorsements, either expressed or implied, of the Air Force Office of Scientific Research or the U.S. Government.

REFERENCES

1. J.-P. Berenger, Three-dimensional perfectly matched layer for the absorption of electromagnetic waves, *J. Comput. Phys.* **127**, 363 (1996).
2. J. M. Jin and W. C. Chew, Combining PML and ABC for finite element analysis of scattering problems, *Micro. Opt. Tech. Lett.* **12**, 192 (1996).
3. N. V. Kantartzis and T. D. Tsiboukis, A comparative study of the Berenger PML, the superabsorption technique and several high-order ABC's for the FD-TD algorithm in two and three dimensional problems, *IEEE Trans. Magn.* **33**, 1460 (1997).
4. L. Zhao and A. C. Cangellaris, GT-PML: Generalized theory of perfectly matched layers and its application to the reflectionless truncation of finite-difference time-domain grids, *IEEE Trans. Microwave Theory Tech.* **44**, 2555 (1996).
5. P. G. Petropoulos, L. Zhao, and A. C. Cangellaris, A reflectionless sponge layer absorbing boundary condition for the solution of Maxwell's equations with high-order staggered finite difference schemes, *J. Comput. Phys.* **139**, 184 (1998).

6. K. S. Yee, Numerical solution of initial boundary value problems involving Maxwell's equations in isotropic media, *IEEE Trans. Antennas Propagat.* **14**, 302 (1966).
7. R. L. Higdon, Radiation boundary conditions for elastic wave propagation, *SIAM J. Numer. Anal.* **27**, 831 (1990).

Received December 2, 1997; revised March 3, 1998

Peter G. Petropoulos
Department of Mathematics
Southern Methodist University
Dallas, Texas 75275
E-mail: peterp@golem.math.smu.edu